University of Michigan — Michigan Engineering

NERS/BIOE 481

Lecture 03
Radiation Sources, X-rays

Michael Flynn, Adjunct Prof
Nuclear Engr & Rad. Science
mikef@umich.edu
mikef@rad.hfh.edu

Henry Ford Health System
RADIOLOGY RESEARCH

III.A - Point Sources of Radiation (11 charts)

A) Radiation Units
1) Units (ICRU)
2) Solid Angle
3) X-ray emission
4) Radiation Exposure

III.A.1 - Units (ICRU)

The International Commission on Radiation Units and Measurements (ICRU) was established in 1925 by the International Congress of Radiology. Since its inception, it has had as its principal objective the development of internationally acceptable recommendations regarding quantities and units of radiation and radioactivity

Name	Symbol	SI unit	Alternate units
'Particle' number	N	1	-
'Particle' flux	$\dot{N}$	s^{-1}	-
'Particle' fluence	Φ	m^{-2}	-
'Particle' fluence rate	$\dot{\Phi}$	$m^{-2}\ s^{-1}$	-
Energy fluence	Ψ	$J\ m^{-2}$	-
Energy fluence rate	$\dot{\psi}$	$W\ m^{-2}$	-
Exposure	X	$C\ kg^{-1}$	Roentgen
Exposure rate	$\dot{X}$	$C\ kg^{-1}\ s^{-1}$	Roentgen/sec
Decay constant	λ	s^{-1}	-
Activity	A	s^{-1}	Becquerel/Curie

See ICRU Report #85a, Oct 2011

III.A.2 - solid angle definition

For physical processes which are naturally described with a polar coordinate system, it is often necessary to identify the fraction of a unit sphere interior to a surface formed by moving the radial vector to form a conic structure. By convention, the entire unit sphere is defined to have 4π steradians.

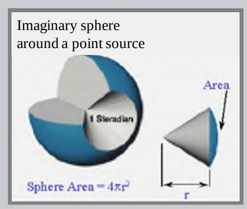

The steradian is the unit used to describe the "solid angle" associated with any portion of the unit sphere.

III.A.2 - differential solid angle

If ϕ is the polar angle from a fixed zenith direction (z) of a spherical coordinate system, and θ is the azimuthal angle of a projection to a plane perpendicular to the zenith (xy), then a differential quantity of solid angle can be written as;

$$d\Omega = \sin(\phi)\, d\phi\, d\theta$$

The $\sin(\phi)$ term is required because of the shorter arc traced by $d\theta$ for angles of ϕ near the poles. The total solid angle of the unit sphere can then be computed by integration of $d\Omega$ to show that this definition of $d\Omega$ leads to the unit sphere having 4π steradians:

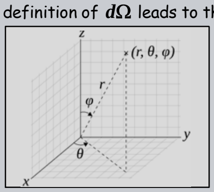

$$\Omega = \int_0^{2\pi}\int_0^{\pi} \sin\phi\, d\phi\, d\theta$$

$$= 2\pi \int_0^{\pi} \sin\phi\, d\phi = 4\pi$$

III.A.2 - fluence in photons/steradian

- Point Sources:
  For sources which emit radiation from a region small enough to be considered a point source, the radiation travels in all directions. Typical radionuclide sources emit radiation with no bias as to the direction and are said to have isotropic emission.
  - For a source which isotropically emits N photons,
  - The fluence is N photons per 4π steradians ($N/4\pi$ photons/sr).
- Fluence at distance r:
  If one considers a sphere with a radius of r mm, this source will produce a fluence of photons traveling through the surface of the sphere equal to:
  - $N/4\pi r^2$ photons/mm^2.
- Fluence Units:
  Radiation fluence can either be expressed in terms of photons/steradian or photons/mm^2. To convert from photons/steradian to photons/mm^2, simply divide by r^2, as seen in the above example.

  photons/mm^2 = (photons/steradian) / r^2, for r in mm

  It is often more convenient to describe the fluence from a source in photons/steradian since it is independent of the distance (i.e. radius) from the emission point.

III.A.2 – directional fluence

- For x-ray sources emitting radiation from a small spot, the intensity of emitted radiation can be different depending on the angle of emission relative to the target surface.

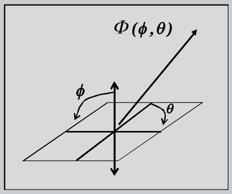

- In this case, the emitted fluence can still be expressed as the quantity of radiation emitted in a small solid angle in the direction (ϕ,θ).
- The fluence, $\Phi(\phi,\theta)$, thus has units of photons/steradian in the emission direction

III.A.3 – X-ray emission

Electron Impact X-ray Source

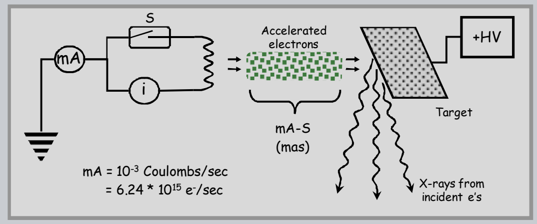

- A high voltage difference (kV or kVp) is established between the filament (cathode) and the target (anode).
- Electrons strike the target with a kinetic energy of To which in electron-volt units (eV or keV) is equal to the kV.
- The production of x-rays is proportional to the number of electrons that strike the target and therefore the mA-S.
- It is thus common to normalize the emission fluence rate as photons/steradian/mA-S or photons/m^2/mA-S.

III.A.3 – X-ray emission

X-ray fluence – differential energy spectrum

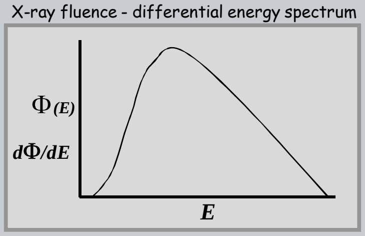

By convention, we will refer to the differential energy spectrum of xray quantities by writing the symbol as a function of energy,

$$\Phi(E) = d\Phi / dE \qquad \Psi(E) = E\Phi(E)$$

Differential particle fluence photons/sr/mA-s/kev

Differential energy fluence ergs/sr/mA-s/kev

III.A.3 – X-ray emission

Integrated X-ray particle/energy fluence

The particle fluence can be obtained by integrating the differential spectrum over all energies.

$$\Phi = \int \Phi(E)dE$$

The energy fluence can be obtained by integrating the product of the differential spectrum and energy over all energies (i.e. the first moment integral).

$$\Psi = \int E\Phi(E)dE$$

III.A.4 – Radiation Exposure – air kerma, ergs/gm

- Radiation exposure, X in coulombs/kg, is a measure of radiation quantity based on the ionization produced in a standard amount of dry air. For SI units, no specific unit is defined and exposure is expressed as coulombs/kg.
- The traditional unit of exposure has been the Roentgen, R, for which the conversion is given by 2.58 x 10^{-4} (C/kg)/R.
- Exposure can be predicted by first computing the energy absorbed in air using the differential radiation energy fluence, $\Psi(E)$ in ergs/cm^2/keV and the linear attenuation coefficient describing the absorption of energy in air, $\mu(E)/\rho$ in cm^2/gm;

$$K_{air} = \int \Psi(E)\frac{\mu_{en}(E)}{\rho}dE, (ergs/gm)$$

This quantity is the air kerma (Kinetic Energy Released per unit Mass).

- The SI unit for absorbed energy per mass is the Gray (Gy).

1 Gy = 1 J/kg = 10^4 ergs/gm

III.A.4 – Radiation Exposure – air μ_{en}

The photon mass attenuation coefficient and the mass energy-absorption coefficient for air from NIST tables based on calculations by Seltzer (Radiation Research 136, 147; 1993).

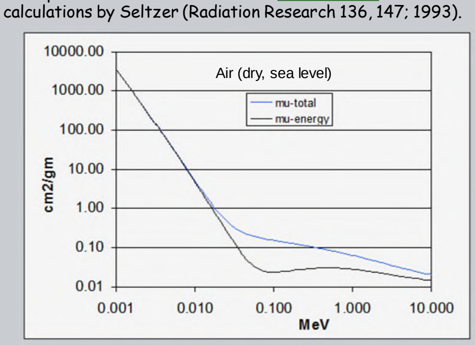

http://physics.nist.gov/PhysRefData/XrayMassCoef/ComTab/air.html

III.A.4 – Radiation Exposure – coulombs/kg (mR)

- The air kerma, K_{air} (ergs/gm), is converted to exposure using a conversion factor of 33.97 Joules/Coulomb (i.e. eV/ion, Boutillon, PMB, 1987);

  Exposure = $K_{air}/(33.97 \times 10^4)$, C/kg (SI unit)

  Exposure = $K_{air}/87.643$, Roentgens (old unit)

- Air kerma, K_{air}, in Gray is now used interchangeably as a measure of radiation exposure.
  - To convert results from units of gray to exposure in milliRoentgens (mR);

    mR = 114.1 mG = μG/8.76
  - To convert results from units of mR to air kerma;

    μG = mR x 8.76

1 J/kg = 10^4 ergs/gm

III.B – Electron impact x-ray tubes (10 charts)

B) Electron Impact X-ray Tubes
1) X-ray generator systems
2) Electron beam
3) Target/Housing Heat.

III.B.1 – X-ray generation systems

Tube - glass or metallic vacuum tube for e- beam.

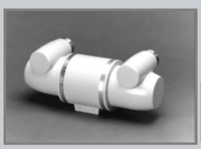

Housing – shielding and cooling.

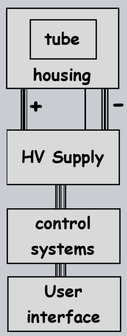

Modern generators use programmed control stations or computer interfaces to quickly select technical factors for a large set of objects and views

Control
- mA
- kV
- Sec

III.B.2 – electron beam

Anode rotation spreads heat input along a long track

- An offset cathode filament emits electrons with a current dependant on temp.
- HV accelerates e^- which strike the target along a line.
- From the side, the emission appears as a square spot.

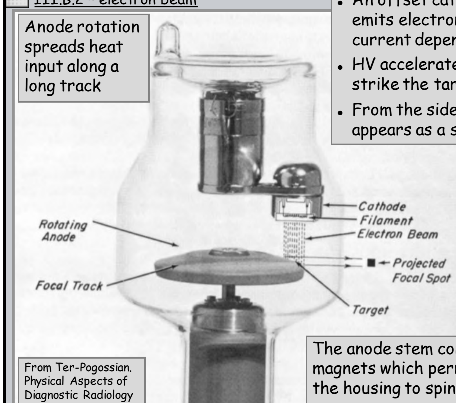

From Ter-Pogossian. Physical Aspects of Diagnostic Radiology

The anode stem contains magnets which permit coils in the housing to spin the target.

III.B.2 – electron beam focus

- The shape of the cup behind the filament bends the electric field lines.
- Electrons are focused towards a spot by the shape of the field lines.
- Some tubes set an additional bias voltage between the cup and the filament to improve focus.

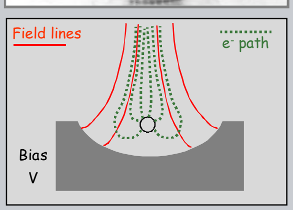

III.B.2 – electron beam current

- Tube current is controlled by varying filament current.
- For the same current and temp., mA increases with kV due to a decrease in the space charge surrounding the filament.

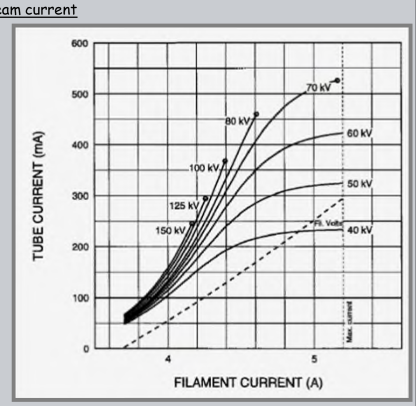

III.B.3 – anode damage

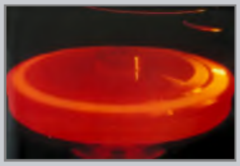

- Watts = kV * mA — 100 kV * 500 mA = 50 kW
- Joules = Watts*Sec — 50 kW * 1 sec = 50 kJ

Anode damage from high instantaneous power (2) and extended heat input (3)

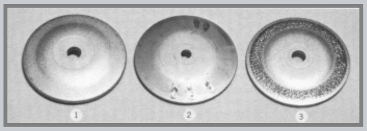

NOTE: The heat unit (HU) was used previously to account for the waveform.
HU = J for a constant potential generator
= 1.4 * J for a single phase generator

III.B.3 – anode power limits

- For a specific xray tube, a rating chart indicates the limits for
  - kV,
  - mA, and
  - exposure time.
- Exceeding the limit causes heat damage along the anode track.

Maximum Exposure Time per Pulse

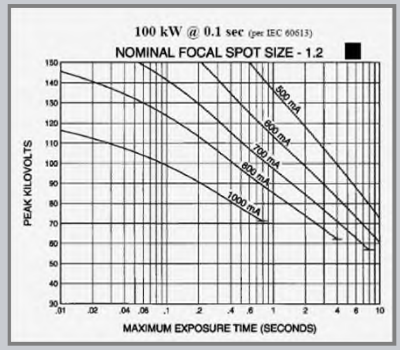

III.B.3 – anode heating/cooling

- For a specific xray tube, a rating chart describes the anode heat (J) storage in relation to input power (watts)
- At the maximum heat capacity, the anode will be at it's maximum temperature.
- A separate curve indicates how heat is dissipated from the anode to the housing.

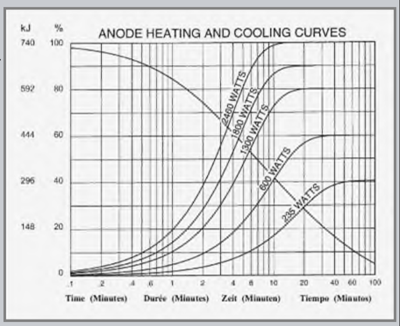

III.B.3 – cooling the tube housing

- Some radiation imaging devices require that the x-ray tube be run at high power for extended times.
  - CT scanner, 100kW ~30 sec
  - Angiography, 120kW 100s pulses
- These systems require excellent heat transfer from the anode to the housing.
- Circulating oil and a heat exchanging transfers heat out of the tube housing.

III.B.3 – Cooled Anode x-ray tube.

Shardt et. al.,Med Phys,31 (9), 2004.

One manufacturer (Siemens) has an x-ray tube where the entire tube body rotates, rather than just the anode, as is the case with conventional designs. This change allows all the bearings to be located outside the evacuated tube, and enables the anode to be cooled more efficiently.

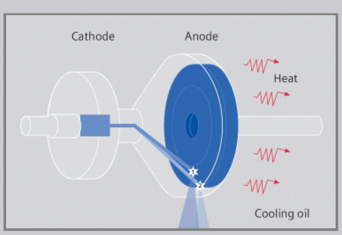

- The Straton has a low inherent heat capacity of 0.8 MHU, but an extremely fast cooling rate of 5 MHU/min (83 kHU/sec).
- This permits continuous scanning with no time limit at 120 kVp and 700 mA.

III.C.1 – X-ray Spectrum – Bremsstralung (14 charts)

C) X-ray Energy Spectrum
1) Bremsstralung (continuous)
2) Characteristic
3) Experimental Spectra
4) Examples

III.C.1 – Bremsstrahlung

- Bremsstrahlung, German for braking radiation, is electro-magnetic radiation produced by the acceleration of a charged particle, such as an electron, when deflected by another charged particle, such as an atomic nucleus.
- An electron gradually looses energy as it slows down in a material. At any point along it's path, a bremsstrahlung photon may be created.

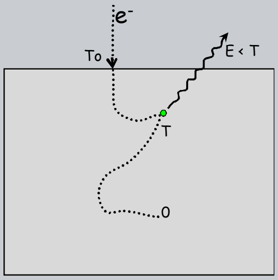

In an individual deflection by a nucleus, the incident particle can radiate any amount of energy from zero up to its total kinetic energy T.

III.C.1 – MC

The track of a single electron is simulated using Monte Carlo software (Penelope). Early in the track, an x-ray is generated (yellow) and escapes from the surface.

Electron transport

- 100 keV
- 10 µm x 5µm
- Tungsten(74)

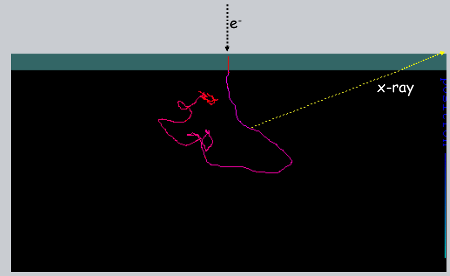

III.C.1.a –Kramers & Kuhlenkampff

In 1923, Hendrik Antonie Kramers (1894-1952) published a significant theoretical paper which included a derivation of the continuum energy spectrum. Kramers began with the quantum theory of Bohr to provide the theoretical basis for his relationship. The paper is one of the first applications of the then new quantum theory to a practical physics problem.

$$\varphi(E_\gamma) = KZ \,{(T_o - E_\gamma)}\big/{E_\gamma}$$

$$\psi(E_\gamma) = E_\gamma \phi(E_\gamma) = KZ(T_o - E_\gamma)$$

E_γ= emitted xray energy

T_o= incident electron energy, i.e. kV

K, phots/keV/mA-s/sr

- K = 6.64 X 10^8 @ 30 keV
- K = 6.31 X 10^8 @ 40 keV
- K = 4.99 X 10^8 @ 180 keV

Note: values based on the interpretation by Sean Hames of text in the original paper.

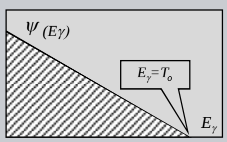

This theoretical result agreed well with the experimental results published by Kuhlenkampff the year before (1922, Ann. Physik)

Kramers HA, On the theory of X-ray absorption and of the continuous X-ray spectrum, Philos. Mag., 46(275):836-871N, Nov. 1923. (Communicated by Prof N. Bohr, Copenhagen)

III.C.1.a – Brems. production efficiency

- Kramer's relationship is easily integrated to compute the total radiative energy produced by a thick target.

$$\int \psi(E_\gamma) dE_\gamma = \int E_\gamma \phi(E_\gamma) dE_\gamma$$
$$= \int_0^{T_o} KZ(T_o - E_\gamma) dE_\gamma$$
$$= \tfrac{1}{2} KZ T_o^{\,2}$$

- Using;
  To = 100 keV and Z = 74
  K = 6 x 10^8 photons/keV/mA-S/sr and 2π steradians (sr)
  the radiated energy is
  E_{rad} = 1.391 x 10^{15} keV/mA-S
- Using 1 mA-S = 6.24 x 10^{15} electrons, this becomes
  E_{rad} = .22 kev/electron
- Since we assumed 100 keV/electron, the efficiency for converting the energy in the electron beam to radiation is 0.2%

III.C.1.b –Brems. Differential Cross Section (DCS)

SLIDE FROM L02

- The probability per atom that an electron traveling with energy T will produce an x-ray within the energy range from E to E+dE is known as the differential radiative cross section, $d\sigma_r/dE$.
- Theoretic expressions indicate that the bremsstrahlung DCS can be expressed as;

$$\frac{d\sigma_r}{dE} = f_r(T,E,Z)\frac{Z^2}{\beta^2}\frac{1}{E}$$

- Where β is the velocity of the electron in relation to the speed of light.
- The slowing varying function, $f_r(T,E,Z)$, is often tabulated as the scaled bremsstrahlung DCS. (SHOWN IN L02)

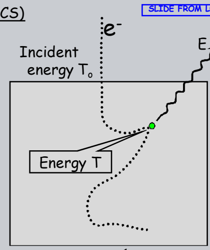

$$\beta^2 = 1 - \frac{1}{(1+\tau)^2}$$

$$\tau = T\big/ m_e c^2$$

Seltzer SM & Berger MJ, Atomic Data & Nucl. Data Tables, 35, 345-418(1986).

III.C.1.b –Integral solution for bremsstrahlung production

- The total radiative production of x-rays with energy in the range from E to E+dE can be found by integrating the production per unit pathlength over the path of the electron.

$$\mu_{rs}(T,E) = N\sigma_r(T,E) = \frac{d\mu_{rs}}{dEdS}$$

$$\mu_{rs}(T,E) = 0,\ T \le E$$

Probability per cm per keV

$$\phi(E) = \frac{d\phi}{dE} = \int_0^{S(E)} \mu_{rs}(T(S),E)dS$$

- Using the electron stopping power, dT/dS, this can be converted to an integration over the energy of the electron as it slows down.

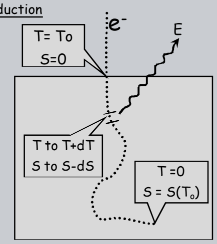

$$\phi(E) = \int_E^{T_o} \frac{\mu_{rs}(T,E)}{dT/dS} dT$$

Xrays/electron/keV

III.C.1.c – A simplified integral solution

- An early quantum-mechanical theory of radiative collisions (Evans, chapter 20) results in the following expression for the radiative DCS.

$$\frac{d\sigma_r}{dE} = \sigma_o B Z^2 \frac{T + m_o c^2}{T} \frac{1}{E}, cm^2 / nucleus$$

$$\sigma_o = \frac{1}{137}\left(\frac{e^2}{m_o c^2}\right)^2 = 0.580, millibarns / nucleus$$

- Where B is a very slowly varying function of Z and the electron energy, T, with a value of approximately 10
- The term $(T+mc^2)/T$ is equal to $0.5/\beta^2$ for small T. This expression is thus consistent with the scaling of the cross shown in the prior slide.
- At values of T small relative to mc^2 and for a constant value of B, this can be used to deduce an approximate expression for the bremsstrahlung spectra.

$$\phi(E) = N_o \frac{\rho}{A} \sigma_o B Z^2 \int_E^{T_o} \left[\frac{m_o c^2}{T} \frac{1}{E}\right] \Big/ \left(dT/ds\right) dT$$

III.C.1.c – Integrating the inverse stopping power

The stopping power can be approximated by an expression proportional to the inverse of the electron energy ($\sim 1/T$);

$$dT/dS = -k_a \left(\frac{Z}{A}\right)\left(\frac{\rho}{T}\right), kev / cm$$

Note: in lecture 2, we saw that a better approximation is $1/T^{0.65}$. We use 1/T now to permit integration.

The integration of the inverse of the stopping power can be used to estimate the pathlength of the electron. For a stopping power proportional to $1/T$, the pathlength is proportional to the incident electron energy squared.

The Thomson-Whiddington law described electron range as proportional to energy squared (Whiddington, Proc. Roy. Soc. London, A86, 1912)

$$S(T_0) = \int_{T_0}^{0} \frac{1}{dT/dS} dT$$

$$S(T_0) = \frac{1}{k_a \rho} \frac{A}{Z} \int_0^{T_0} T dT$$

$$S(T_0) = \left(\frac{1}{k_a \rho} \frac{A}{Z}\right) T_0^{\,2}$$

III.C.1.c – Equivalent Kramers model

- Using the approximation that the stopping power can be approximated by an expression proportional to $1/T$,

$$dT/dS = k_a \left(\frac{Z}{A}\right)\left(\frac{\rho}{T}\right), kev / cm$$

- The simplified integral solution evaluates to an expression essentially the same as Kramer's equation,

$$\phi(E) = N_o \frac{\rho}{A} \sigma_o B Z^2 \int_E^{T_o} \left[\frac{m_o c^2}{T} \frac{1}{E}\right] \Big/ k_a \left(\frac{Z}{A}\right)\left(\frac{\rho}{T}\right) dT$$

$$\phi(E) = \frac{N_o \sigma_o B}{k_a} m_o c^2 Z \frac{1}{E} \int_E^{T_o} dT$$

$$\phi(E) = \left[\frac{N_o \sigma_o B}{k_a} m_o c^2\right] Z \frac{T_o - E}{E}, xrays / electron / keV$$

- Where,

$$\frac{k_e}{4\pi}\left[\frac{N_o \sigma_o B}{k_a} m_o c^2\right] = 6.67E08, xrays / mAS / keV / sr$$

This is equivalent to Kramers!

See 'Flynn L03b' on course website

III.C.1.d – Self Absorption

- X-rays produced at some depth within the target that have a very low energy, are frequently absorbed within the target.
- One approach to account for this self-absorption is to include a term within the integral solution describing the probability of escape to x-rays of energy E produced by electrons of energy T.

$$\phi(E) = \int_E^{T_o} \frac{\sigma_{rs}(T,E)}{dT/dS} F_a(E,T) dT$$

- In an integral solution using;
  - improved B in the cross section
  - improved stopping power

  The self absorption term has been computed by considering the mean depth of electron penetration.
  - $\phi(E)E$ (Kramers)
  - $\phi(E)E$ (integral)

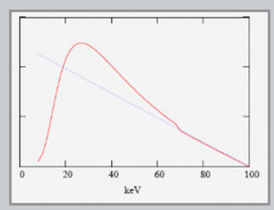

See 'Flynn L03b' on course website

III.C.1.d – Intrinsic Absorption

- The attenuation by the internal materials of the tube and housing is significant below about 40 keV for general radiography tungsten target tubes. This is commonly referred to as 'intrinsic filtration'.
- The effect of intrinsic filtration on the energy fluence spectrum is seen to further reduce low energy emissions such that the spectrum is similar to Kramer's equation above 40keV.
  - $\phi(E)E$ (Kramers)
  - $\phi(E)E$ (integral)

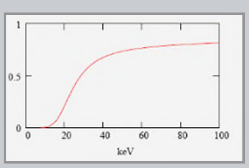

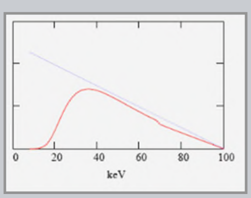

See 'Flynn L03b' on course website

III.C.1.e – Prior integral bremsstrahlung models

- Kramers HA, Philos. Mag. 46(275) 1923.
  Semi-classical DCS, 1/T dT/dS, no absorption
- Storm E, Phys. Rev. A 5(6) 1972.
  Born/Sommerfield DCS, Berger&Seltzer dT/dS, fixed depth
- Birch & Marshall, Phys. Med. Biol. 24(3) 1979.
  polynomial DCS, Bethe dT/dS, T-W penetration
- Tucker et.al., Med. Phys., 18(2&3) 1991.
  Polynomial DCS, Berger&Seltzer dT/dS, T-W penetration

- For these integral models, electron transport effects (backscatter, absorption, angular distributions) are approximated by simple expressions.
- Dodge has recently developed an advanced integral model (WSU 2008) that uses electron transport distributions determined from Monte Carlo simulations.

III.C.1.e – The Storm model (xspect 3.5)

- A notable work on the modeling of the continuous spectrum was published by Storm in 1972 (Storm, Phys. Rev. A, 5(6):2328-2338, June 1972).
- Storm formally evaluated several cross sections detailed by Koch and Motz (ref 2). These cross sections have more validity than the Compton and Allison cross section used by most other investigators. He shows that for spectral estimation the best fit to experimental data is obtained with a differential (in energy) cross section derived using the Born approximation with no screening (3BN).
- He then presented a mathematical fit for the bremsstrahlung intensity which specifically accounts for electron backscatter.

$$\Psi(E_\lambda) = \left(\frac{11}{4\pi} Z \frac{(T_o - E_\lambda)\left(1 - e^{-3E_\lambda / E_K}\right)}{(E_\lambda / T_o)^{1/3}\left(1 - e^{-T_o / E_K}\right)} \right) f_a$$

The Storm model is used to compute the bremsstralung spectrum in xSpect 3.5 used in the NERS 580 computational lab course. The Dodge model is to be used in xSpect 4.0 (yet to be released).

$\Psi(E\gamma)$ = diff. energy fluence
$E\gamma$ = emitted x-ray energy
T_o = electron energy (high voltage)
E_K = K binding energy
f_a = self absorption

III.C.1.e – xspect accuracy

xspect 3.5 and xspect 4.0 in relation to Mercier experimental

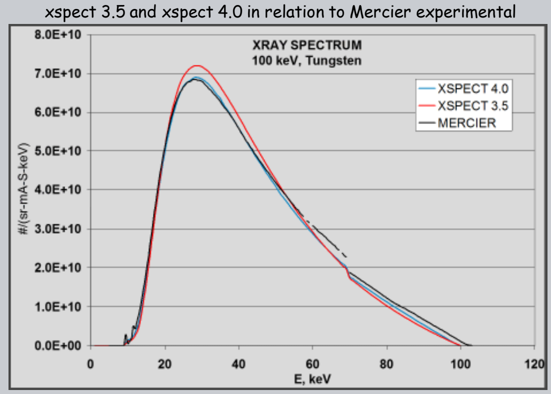

 * XSPECT 4.0, normalized values

III.C.2 – X-ray Spectrum – Characteristic (13 charts)

C) X-ray Energy Spectrum
1) Bremsstralung (continuous)
2) Characteristic
3) Experimental Spectra
4) Examples

III.C.2 – Characteristic Radiation Production

The emission of radiation with energies characteristic of the target material results from atomic shell transitions that occur as a result of a vacancy created in an inner shell, usually the K or L shell.

- Direct production:

  As each electron penetrates into the target, shell vacancies are occasionally produced by electron-electron interactions in the atoms of the target material.
- Indirect production:

  Additionally, many of the bremsstralung x-rays produced by electron-nucleus interactions are absorbed in the target by photo-electric interactions which result in shell vacancies, primarily the K shell.

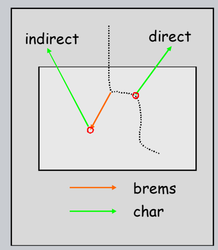

III.C.2 – Characteristic Direct vs Indirect, Green and Cosslett 1961

"Direct and indirect production are calculated and the ratio of indirect to total production is shown to be in agreement with experimental results .."

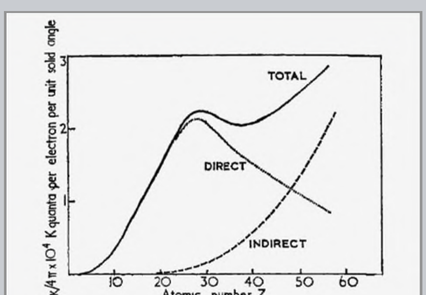

Fig. 4. K quanta per electron per unit solid angle at $U_0 = 3$.

The overvoltage, U_0 , is the ratio of the incident electron energy, T_0, to the K binding energy, E_K; $U_0 = T_0/E_K$

III.C.2 –Characteristic Atomic levels

SLIDE FROM L02

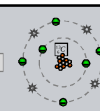

- Each atomic electron occupies a single-particle orbital, with well defined ionization energy. https://en.wikipedia.org/wiki/X-ray_notation
- The orbitals with the same principal and total angular momentum quantum numbers and the same parity make a shell.

Each shell has a finite number of electrons, with ionization energy Ui.

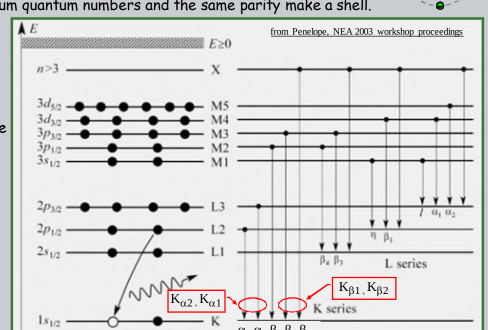

III.C.2 – Characteristic Energies

NIST X-ray Transition Energy Database

Material	Z	$K_{\alpha 2}$	$K_{\alpha 1}$	$K_{\beta 2}$	$K_{\beta 1}$
Cr	24	5.40	5.41	6.00	5.95
Y	39	14.88	14.96	17.01	16.74
Mo	42	17.37	17.48	19.96	19.61
Rh	45	20.07	20.22	23.17	22.72
W	74	57.98	59.32	69.07	67.25
Pt	78	65.12	66.83	77.83	75.75
		K-L2	K-L3	K-N2,3	K-M3

X-ray notations vary in the literature.

$K_{\alpha 2}$ is the Siegbahn notation. K-L2 is the IUPAC notation.

III.C.2 – K fluoro x-ray energies

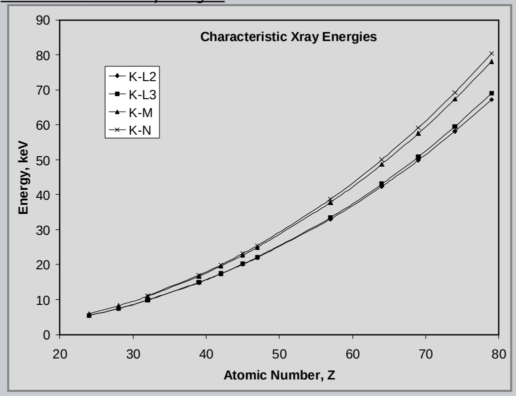

Derived from the LLNL Evaluated Atomic Data Library (EADL), Perkins, Cullen, Chen, et. al. (1991).

III.C.2 – Atomic relaxation

SLIDE FROM L02

- Excited ions with a vacancy in an inner shell relax to their ground state through a sequence of radiative and non-radiative transitions.
- In a radiative transition, the vacancy is filled by an electron from an outer shell and an x ray with characteristic energy is emitted.
- In a non-radiative transition, the vacancy is filled by an outer electron and the excess energy is released through emission of an electron from a shell that is farther out (Auger effect).
- Each non-radiative transition generates an additional vacancy that in turn, migrates "outwards".

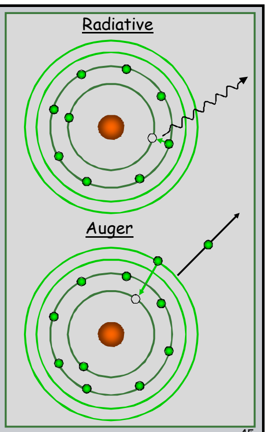

III.C.2 – K fluoro transition probabilities

SLIDE FROM L02

Relative probabilities for radiative and Auger transitions that fill a vacancy in the K-shell of atoms.

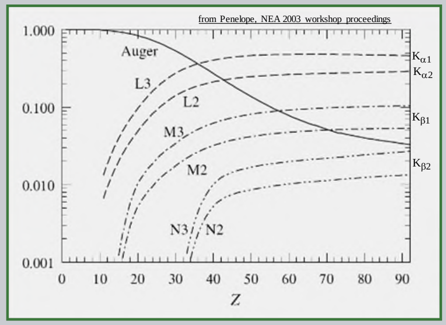

III.C.2 – Fluorescent fraction

The fluorescent yield (char. x-ray emission) has been approximated by polynomial expressions.

Total K shell fluorescent yield versus atomic number

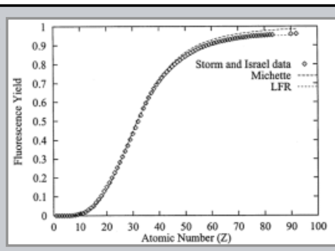

Michette ;

$$\omega_K = \frac{Z^4}{Z^4 + 1.12E06}$$

Laberrique-Frolow & Radvany LFR, 1956 ;

$$\omega_K = \frac{\left(A + BZ + CZ^3\right)^4}{1 + \left(A + BZ + CZ^3\right)^4}$$

$A = -0.0217$
$B = 0.03318$
$C = -1.14E\text{-}06$

III.C.2 – K fluoro transition probabilities

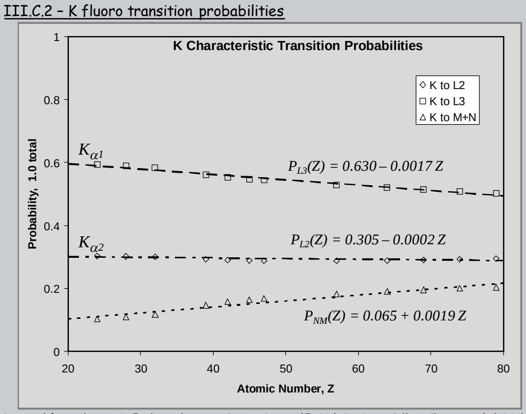

Derived from the LLNL Evaluated Atomic Data Library (EADL), Perkins, Cullen, Chen, et. al. (1991).

III.C.2 – Characteristic KL production, Storm 1972

"Webster and Clark were the first of many investigators to report that the K-photon intensity could be described by an empirical formula of the form"

$$\phi_K = C_K(T_O - E_K)^{\eta_K}$$

"The present calculation indicates this formula is good for tungsten up to values of E_O-70 = 100 kV with"

$C_K = 4.25 \times 10^8$

$\eta_K = 1.67$

"And C_K in units of photon/(sec mA sr)."

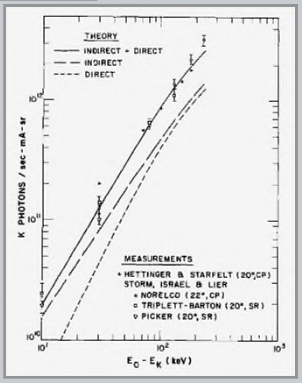

- Storm, J. Appl. Phys., Vol. 43, No. 6, June 1972
- Webster, Proc. Natl. Acad. Sci. US, 3, 181 (1917)

III.C.2 – Characteristic Radiation Theory, Green and Cosslett 1961

Green and Cosslet proposed a simple theoretical expression is for K quanta production. Total production is expressed as a function of Z and overvoltage Uo. The fluence is proportional to;

$$(U_0 - 1)^{1.67}$$

The overvoltage U_o is T_o/E_K and so $U_0 - 1 = (1/E_K)(T_o - E_K)$

Experimental work referred to by Compton and Allison (1935) suggested values of the power of U_0-1 of 1.65.

The total K production per electron per steradian is given by Green and Cosslett as;

$$N_K/4\pi = \omega_k(2.8 \times 10^3 R/Ac + 4.27 \times 10^{-10} (Z-2)^2 Z)(U_0-1)^{1.67}$$

with ω_k given by the LFR polynomial expression.

GREEN and COSSLETT, 1961, Proc. Phys. Soc., 78, pg 1206

III.C.2 Experimental Production, Green 1968

- In 1968, Green and Cosslett reported the results of experimental measurements of the production of K and L characteristic radiation for numerous elements.
- Straight line fits indicated that the efficiency of production is proportional to;

$$(U_o - 1)^{1.63}$$

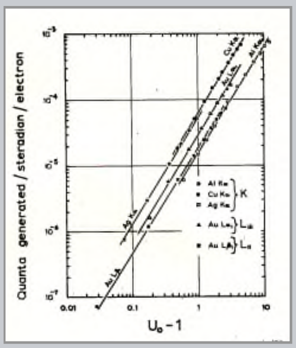

GREEN and COSSLETT, 1968, Brit. J. Appl. Phys., Vol. 1, ser. 2

III.C.2 Experimental Production, Green 1968

Green and Cosslett reported the experimental values of efficiency were reported in relation to Z for functions of either $(U_o - 1)^{1.63}$ or $(T_o - E_x)^{1.63}$.

- xSpect 3.5 uses empiracle relations of the form $C(T_o - E_k)^n$. Values for C and n are only availabe for tungsten and molybdenum targets.
- xSpect 4.0 uses polynomials developed by Dodge (WSU 2008) that are function of Z, T_o and target takeoff angle.

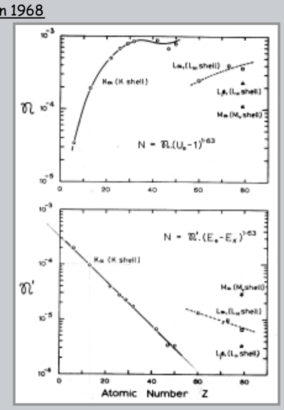

GREEN and COSSLETT, 1968, Brit. J. Appl. Phys., Vol. 1, ser. 2

III.C.3 – X-ray Spectrum – Experimental (5 charts)

C) X-ray Energy Spectrum
1) Bremsstralung (continuous)
2) Characteristic
3) Experimental Spectra
4) Examples

III.C.3 - Experimental Spectral Data

Experimental Spectral Data

- Limited data is available for specific targets, takeoff angle, and tube filtration
- Difficult to accurately measure.
  - Complicated detector response corrections.
  - Absolute intensity determined from exposure
  - Actual intrinsic filtration uncertainty.
  - Target surface roughness effects.

III.C.3 - X-ray Spectra – Experimental Data

--- US FDA ---

- Fewell & Shuping, FDA 81-8162 (1981)
  Tungsten, glass, 70-140 kV
- Fewell & Shuping, FDA 79-8071 (1978)
  Tungsten & Molybdenum, glass+, 20-60 kVp
- Fewell, Jennings & Quinn, BRH/CRDH (1991, 1994)
  Tungsten, Molybdenum & Rhodium
  18-42 (every 2) kV, ~.5mm Be

Algorithms to interpolate FDA experimental Data:

- Boone & Seibert, Med. Phys., 24(11),1997
  - TASMIP – tungsten
- Boone, Fewell & Jennings, Med. Phys., 24(12),1997
  - RASMIP – rhodium
  - MASMIP - molybdenum

(Note: Data normalized to new mR/mA-s measures)

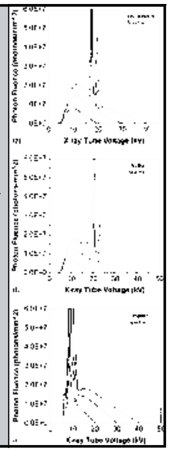

III.C.2 – Characteristic KL production, Mo

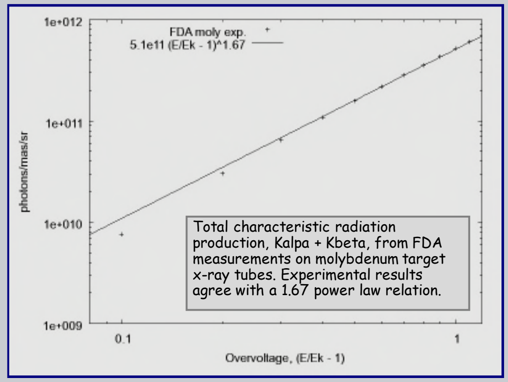

Total characteristic radiation production, Kalpa + Kbeta, from FDA measurements on molybdenum target x-ray tubes. Experimental results agree with a 1.67 power law relation.

III.C.3 - X-ray Spectra – Experimental Data

- Mercier, Radiation Research 154, 564–581 (2000)
  - Tungsten, 20°, 7 mm Be
    – 80, 90, 100, 120, 150 kV
  - Tungsten, 12°, Glass/oil/Al
    - 30, 50, 60, 70 kV
  - HP-Ge & CZT spectrometers, MC based response corrections

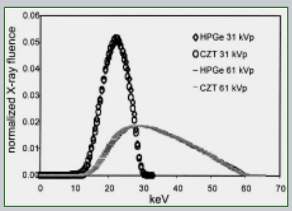

Tabulated x-rays/mAs·cm2 at 1 m in 0.5-keV energy bins

Tube μGy/mAs at 1 m EPPT (± 0.1 μm) keV	Isovolt[a] 336.4 1.4 μm 151.8 kVp	Isovolt[a] 264.3 1.3 μm 122.3 kVp	Isovolt[a] 215.1 1.2 μm 101.5 kVp	Isovolt[a] 206.2 1.15 μm 92.8 kVp	Isovolt[a] 177.5 1.1 μm 82.4 kVp
50.5	3.62×10^{8}	2.74×10^{8}	2.06×10^{8}	1.84×10^{8}	1.44×10^{8}
51.0	3.58×10^{8}	2.71×10^{8}	2.03×10^{8}	1.81×10^{8}	1.42×10^{8}
51.5	3.56×10^{8}	2.68×10^{8}	2.00×10^{8}	1.77×10^{8}	1.39×10^{8}
52.0	3.52×10^{8}	2.64×10^{8}	1.97×10^{8}	1.73×10^{8}	1.37×10^{8}
52.5	3.49×10^{8}	2.62×10^{8}	1.94×10^{8}	1.70×10^{8}	1.34×10^{8}
53.0	3.46×10^{8}	2.59×10^{8}	1.91×10^{8}	1.67×10^{8}	1.31×10^{8}
53.5	3.44×10^{8}	2.56×10^{8}	1.88×10^{8}	1.64×10^{8}	1.28×10^{8}
54.0	3.40×10^{8}	2.53×10^{8}	1.85×10^{8}	1.61×10^{8}	1.26×10^{8}
54.5	3.37×10^{8}	2.50×10^{8}	1.82×10^{8}	1.58×10^{8}	1.23×10^{8}
55.0	3.34×10^{8}	2.47×10^{8}	1.79×10^{8}	1.55×10^{8}	1.21×10^{8}
55.5	3.30×10^{8}	2.44×10^{8}	1.76×10^{8}	1.52×10^{8}	1.18×10^{8}
56.0	3.27×10^{8}	2.41×10^{8}	1.74×10^{8}	1.50×10^{8}	1.16×10^{8}

III.C.3 - X-ray Spectra – Experimental Data

- Da Zhang, Medical Physics 39(6), 3493–3500 (2012)
  - Tungsten, 16°, no added filtr.
    – 20-49 kV
  - Amptek X-123 CdTe Spectrometer.

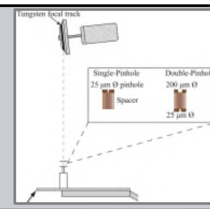

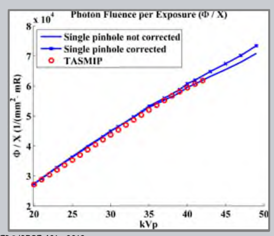

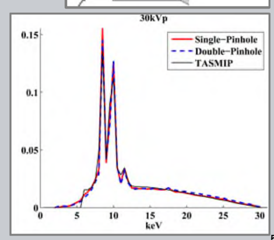

III.C.3 – X-ray Spectrum – Examples (8 charts)

C) X-ray Energy Spectrum

1) Bremsstralung (continuous)
2) Characteristic
3) Experimental Spectra
4) Examples

III.C.3 – X-ray spectral filtration

- X-ray sources typically consist of a vacuum tube mounted in a tube housing with added filtration at the exit port.
- The differential x-ray spectrum is modified by;
  - Target self absorption
  - Attenuation by various material layers

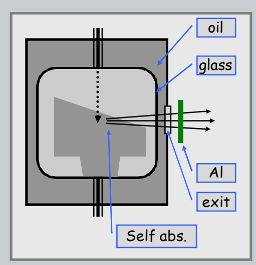

Typical Molybdenum target source
- 0.8 mm Beryllium
- 0.030 mm added Mo

Typical Tungsten target source
- 1.48 mm pyrex glass
- 3.0 mm oil
- 2.5 mm added Al

III.C.3 – Z = 74, 70 kV

Tungsten target, 70 kV, glass tube, oil housing

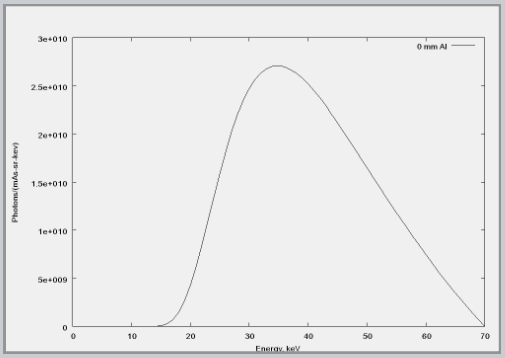

III.C.3 – Z = 74, 70 kV

Tungsten target, 70 kV, glass tube, oil housing

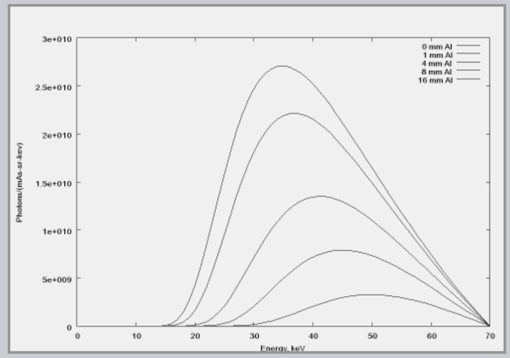

III.C.3 – Z = 74, 120 kV

Tungsten target, 120 kV, glass tube, oil housing

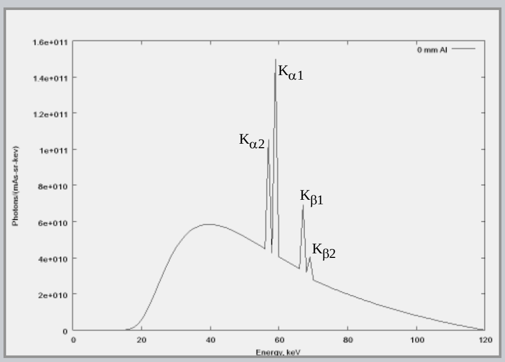

III.C.3 – Z = 74, 120 kV

Tungsten target, 120 kV, glass tube, oil housing

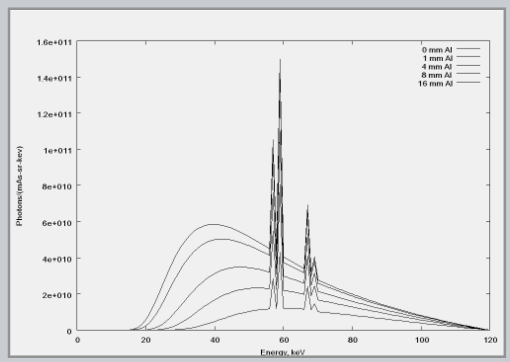

III.C.3 – Z = 42, 34 kV

Molybdenum target, 34 kV, Be window

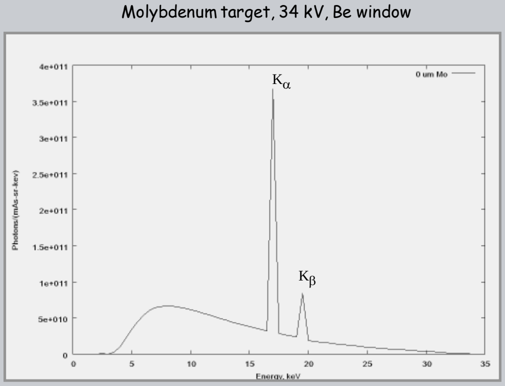

III.C.3 – Z = 42, 34 kV

Molybdenum target, 34 kV, Be window

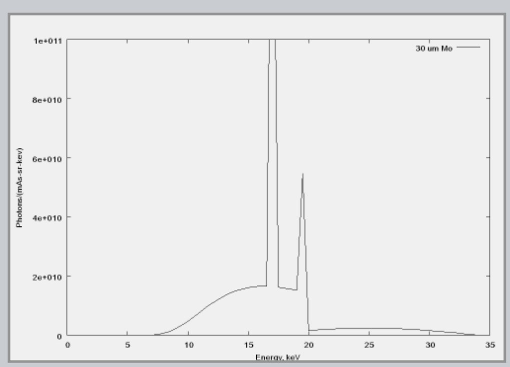

Dual Energy Chest

A linear combination of two images obtained with different kV and added filtration can emphasis either bone or tissue materials

- Dual Energy digital chest radiography can improve nodule detection by removing overlying bone signals.
- Key to the method is the ability to obtain two images very rapidly.

Images from GE Medical Systems (Web)

III.D – Other X-ray Sources (13 charts)

D) Other X-ray Sources
1) Novel cathodes
2) Megavoltage sources (Linac)
3) Synchrotron sources

III.D.1 – Field Emitter Cathode (FEC)

- Electron field emission (FE) occurs for sharply pointed emitters place in an electric field.
- FE devices can be used as unheated cathodes (i.e. cold cathodes).
- X-ray sources using arrays of field emitter cathodes have been proposed for inverse geometry computed tomography.

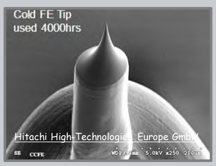

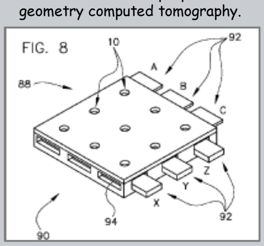

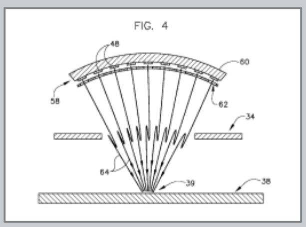

Zou et.al. ; Field Emitter Based Electron Source for Multiple Spot X-ray. US7809114 (2010).

III.D.1 – Field Emitter Cathode

MIT FE X-ray source

Microsystems Technology Lab.

A facility has been built to generate X-rays with an FE cathode and a gold transmission anode. Using the facility, an X-ray absorption image of an ex-vivo sample clearly shows soft tissue and fine bone structures.

The cathode contains arrays of gated field emitters that transmit 99.5% of the electrons to the anode. It has a maximum current of 1.2 μA per field emitter (588 μA total array current).

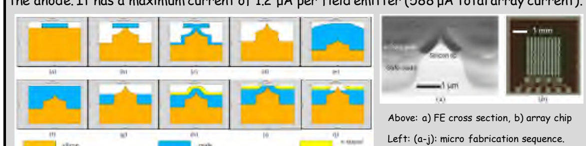

Above: a) FE cross section, b) array chip

Left: (a-j): micro fabrication sequence.

Cheng et.al. ; A Compact X-ray Generator Using a Nanostructured Field Emission Cathode and a Microstructured Transmission Anode, Journal of Physics: Conference Series 476 (2013).

III.D.1 – Carbon Nanotube Cathode

http://www.xintek.com/

Advantages for Carbon Nanotube (CNT) emitters:
- little heat is generated permitting a small X-ray tube size;
- Easy to control for pulsed operation;
- high current density.

Field emission occurs from the ends of numerous nanotubes on the cathode surface.

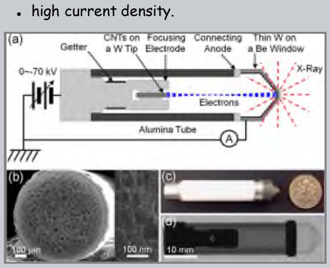

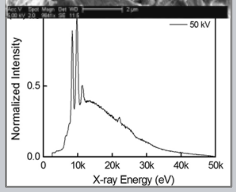

Heo SH, Kim HJ, Ha JM, Cho SO; A vacuum-sealed miniature X-ray tube based on carbon nanotube field emitters, Nanoscale Research Letters (2012).

III.D.1 – Carbon Nanotube Cathode

XINRAY systems http://xinraysystems.com/

Gidcumb et. al., Carbon nanotube electron field emitters for x-ray imaging of human breast cancer, Nanotechnology 25 (2014).

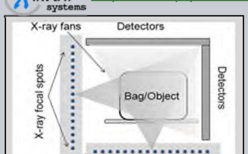

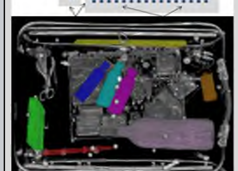

Gonzales et. al., Rectangular Fixed-Gantry CT Prototype: Combining CNT X-Ray Sources and Accelerated Compressed Sensing-Based Reconstruction, IEEE access 2, (2014).

III.D.1 – Pyroelectric Generation of X-rays

Investigations of pyroelectric generation of x rays

Brownridge JD & Raboy S; J. Applied Physics (1999)

Experiments to study .. Crystals such as $LiTaO_3$, $LiNbO_3$, and $CsNO_3$ are discussed.

- During increasing temperature and at appropriate pressures electrons in the vacuum system are accelerated to the +z base of the pyroelectric crystal and are repelled from the -z base of the crystal.
- The electrons striking the crystal may have sufficient energy to excite x-ray absorption edges of the elements in the crystal and the electrons repelled to a target may have sufficient energy to excite x-ray absorption edges in the elements of the target.

The method was commercialized by Amptek in 2003

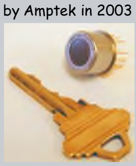

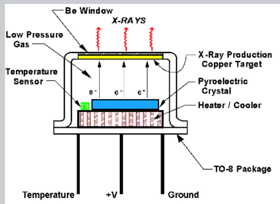

III.D.1 – Pyroelectric Generation of X-rays

Used with a small spectrometer, the x-ray source provides a method for x-ray fluorescent analysis of small specimens.

http://www.amptek.com/coolx.html

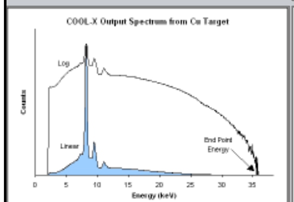

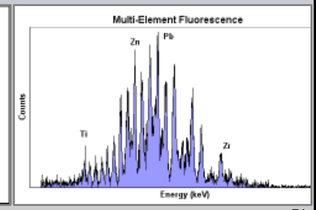

III.D.2 – LINAC

Linear Accelerator (LINAC)

Basic operation

1) An RF system produces oscillating electric fields in the gaps between electodes
2) Charged particles are injected in bunches timed such that they are accelerated by the field.
3) When the field is reversed, the particles are hidden in the bore of the drift tube.
4) The drift tube length and spacing increases to keep pace with the increasing particle velocity.
5) The beam is focused by strong permanent magnet quadrupoles inside each drift tube.

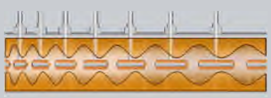

http://www.jpaw.com/

III.D.2 – Medical Linear Accelerator

Megavoltage linear accelerators provide x-ray for radiation therapy with typical peak voltage 4-6 MV.

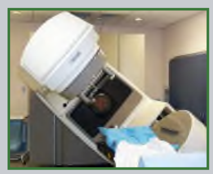

III.D.3 – Synchrotron Sources

By the end of the 19th century, it was understood by a few prominent physicists that any charge which is submitted to an acceleration must radiate some electromagnetic radiation and therefore lose energy.

- Such radiation is called bremsstrahlung when the accelerating field is electric.
- It is called synchrotron radiation when the accelerating field is magnetic in origin.

Undulator

1. Magnets
2. electron beam
3. Synchrotron radiation

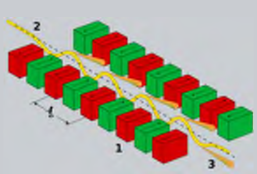

III.D.3 – Synchrotron Sources

Schematic diagram of an energy recovery linac source of synchrotron radiation. A bright electron source injects electrons into a superconducting radio frequency cavity that accelerates electrons to full energy of 5 GeV (the green balls 'surfing' on the crest of the RF travelling wave). They circulate around a return arc producing brilliant x-ray beams in undulators (shown as red rectangles).

The circumference of the arc is adjusted so that the path length of the electrons returning to the linac is 180° out of accelerating phase. Thus these returning (red ball) electrons ride in the trough of the RF wave and now give up their energy to the cavity. After being decelerated to low energy they are directed to a beam dump. Each electron makes one trip around the loop and its energy is recycled in the main linac, hence the name, energy recovery linac

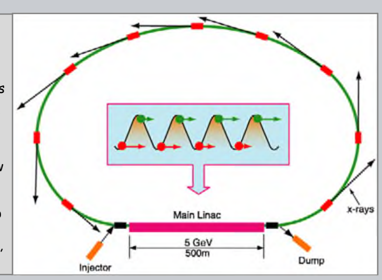

Bilderback, J of Physics B, May 2005

To date there exist more than 50 synchrotron radiation sources in operation in the world serving many areas of science ranging from chemistry, biology, physics, material science, medicine to industrial applications. These facilities are generally government owned laboratories at which many beam lines are dedicated to various scientific endeavors.

Advanced Photon Source (APS), Argonne IL, USA

Notable characteristics of synchrotron x-ray sources include:

- High flux
- Narrow bandwidth
- Small angular divergence

Brilliance (the flux per unit area per unit solid angle of the radiation cone per unit spectral bandwidth) is used to compare different devices.

The radiation is coherent in that it is capable of producing observable interference and diffraction effects.

See Margaritondo2003 (course web site) on the physics of synchrotron production and a discussion of coherence and radiography

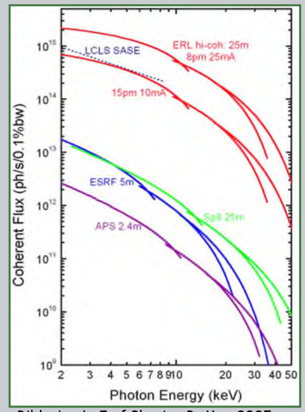

Bilderback, J of Physics B, May 2005

http://cuos.engin.umich.edu

- The Center for Ultrafast Optical Science at the University of Michigan has demonstrated a table top source of bright, ultrafast, coherent synchrotron radiation.
- The x-ray source is based on focusing a pulsed high power laser into a millimeter-sized plume of helium gas, which is immediately ionized and turned into a plasma.
- As the laser propagates through the plasma, it drives an electron density oscillation (plasma wave) with phase velocity ~c in its wake.
- The ponderomotive force of the laser displaces electrons from the almost stationary ions, setting up large accelerating fields.

Nature Physics, v 6, Dec 2010

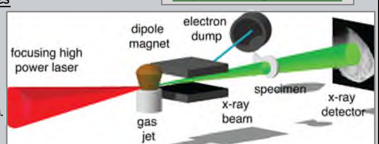

A high power laser is focused into a tenuous gas jet, creating a plasma wave, which serves as a miniature plasma wiggler for the accelerated electrons. The emerging electron and x-ray beam are separated with a magnet. The x-ray beam can be used to image specimens.

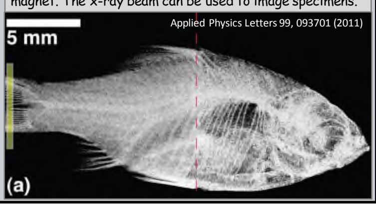

Applied Physics Letters 99, 093701 (2011)